CRREL

Variation in Visual and Near-Infrared Contrast with a Snow Background

Lindamae Peck

August 1994

DTIC
S ELECTE
JAN 1 3 1995
G
D

19950112 044

Abstract

Visual and near-infrared concealment against a snow cover are considered in terms of the daily and longer-term variation in albedo of a shallow (≤26 cm) snow cover. Examples of albedo of a Vermont snow cover demonstrate the influence of time of day (solar angle), incident solar radiation, snow depth, and snow wetness. Most albedos fell within the range 0.75–0.98. The most consistent variation was a decrease in albedo during the morning as the sun angle increased and a corresponding increase with decreasing sun angle in the afternoon. Albedo was low when the snow surface temperature indicated melting was occurring or when an increase in temperature of the soil beneath the snow cover indicated solar radiation was being absorbed by the soil. Examples of the diurnal variation in sun angle and the seasonal variation in maximum potential solar radiation, as calculated from site latitude and longitude and calendar date, are presented.

Special Report 94-28

**U.S. Army Corps
of Engineers**
Cold Regions Research &
Engineering Laboratory

Variation in Visual and Near-Infrared Contrast with a Snow Background

Lindamae Peck

August 1994

Accesion For		
NTIS CRA&I	☒	
DTIC TAB	☐	
Unannounced	☐	
Justification		
By		
Distribution /		
Availability Codes		
Dist	Avail and / or Special	
A-1		

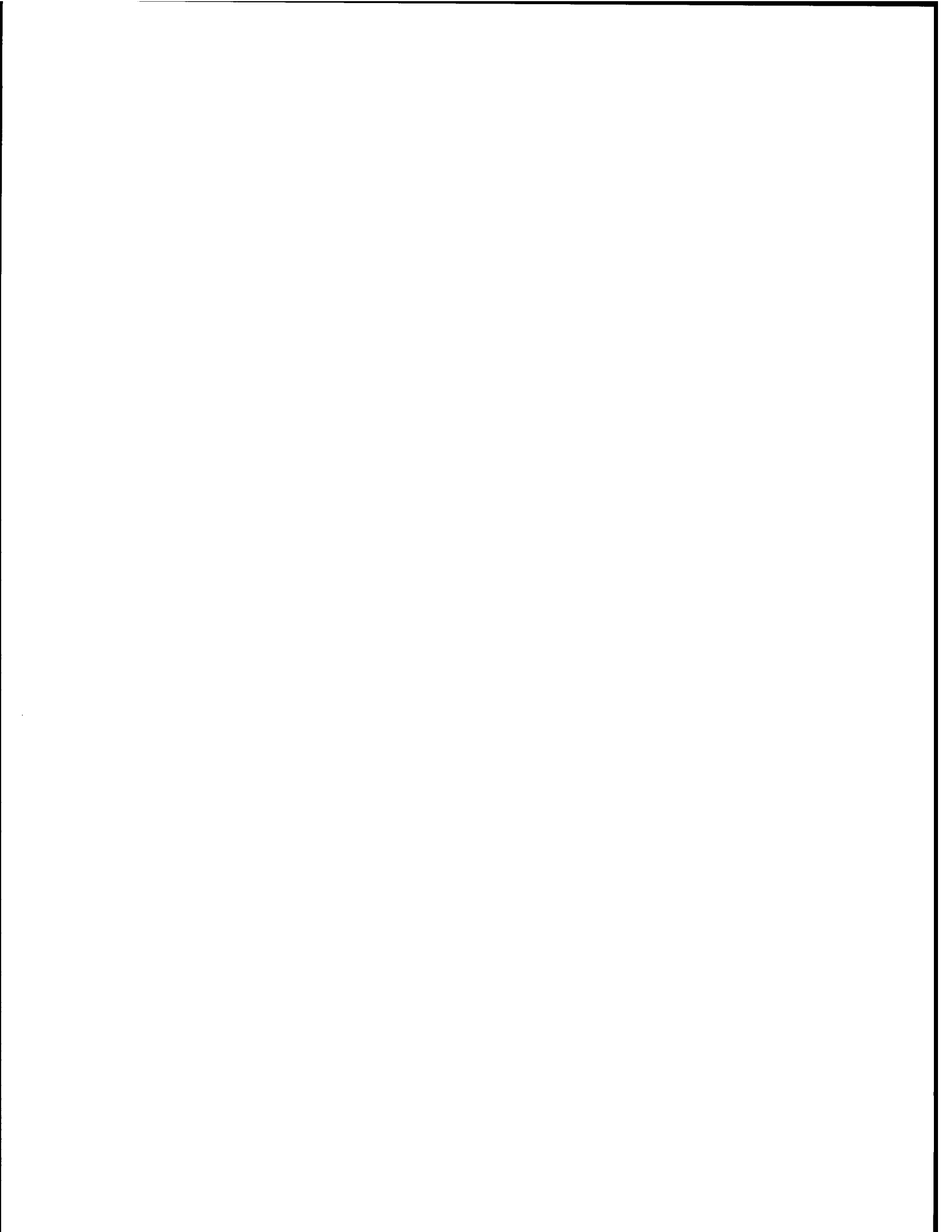DTIC QUALITY INSPECTED 3

19950112 044

PREFACE

The contents of this report are not to be used for advertising or promotional purposes. Citation of brand names does not constitute an official endorsement or approval of the use of such commercial products.

CONTENTS

ILLUSTRATIONS

Variation in Visual and Near-Infrared Contrast with a Snow Background

LINDAMAE PECK

INTRODUCTION

A "white" object viewed against a snow cover under natural illumination typically has a variable visual contrast (Fig. 1). This may in part be due to changes in the reflective properties of the white object during its exposure to the weather. More certainly changes in the illumination and in the physical properties of the snow cover are occurring. Unless the light reflected from the white object also changes to compensate exactly for the change in reflected light from the snow background, the white object will be more or less visible to an observer.

Whether a white object may be visually distinguished against a snow background is an important consideration in exterior security applications. A security guard relies upon an imperfect visual match to detect the presence of an intruder in a restricted area. The intruder attempts to reduce his visual contrast below the guard's perception level through concealment techniques. The guard's task of spotting the intruder is often made easier through the use of surveillance cameras and video motion detection systems. The latter typically digitize the camera scene, convert it to a gray-scale representation, examine subsequent scenes for changes thought to be characteristic of an intruder's motion, and highlight the corresponding portion of the scene. Whereas the guard's eyes are sensitive to the visible spectrum (0.43–0.69-μm wavelengths), the electronic detectors used in cameras may be sensitive over a broader band of wavelengths to include the near-ultraviolet and a portion of the near-infrared. Depending on the imaging device, the spectral response of an exterior camera used for security purposes may range from ~0.35 to 1.1–1.2 μm. Although this makes use of a larger portion of the spectrum of solar illumination (Appendix A), the magnitude of reflected light from a snow cover is more variable at near-infrared wavelengths (Appendix B).

With or without this electronic assistance, the guard makes the final assessment of whether an intruder is present based on what he sees. How well the intruder reduces his visual contrast directly affects the success of his intrusion.

This report provides guidance on the design of detection verification trials for use when visual systems, such as surveillance cameras, video motion detection systems, or human observers, are viewing a snow-covered background. It evaluates the factors determining the visual detection of an object against a snow background. It presents the variation in albedo of a shallow (15- to 26-cm-deep) snow cover over a two-week period at a CRREL field site (SOROIDS) in Vermont to illustrate changeability in light reflected from a snow cover. Because differences in visual and near-infrared contrast with a snow cover arise from changes in natural illumination and in snow-reflective properties, this report presents general examples of the daily and seasonal variation in solar illumination during the northern hemisphere winter, as well as specific examples from SOROIDS. It also summarizes the variation in snow albedo (the ratio of reflected to incident solar radiation) that results from aspects of the illumination, such as sun angle (angle between horizon and sun) and direct sunlight vs. diffuse skylight, and from changes in the snow cover as it ages.

VISUAL CONTRAST

The visual contrast of an object with its background is determined primarily by their difference in brightness. Light is reflected or emitted by the object and background and propagates to an observer. If the observer perceives a difference in the amount of light incident at his location, he visually distinguishes the object from its background. The visual contrast at the observer is dependent on both the difference in brightness between the object and its background at its location (inherent contrast) and on the loss of brightness due to absorption and scattering of light along the propagation path from the object to the

(a) 13 February.

(b) 2 March.

Figure 1. Photos of white objects against a snow cover at 1530 hr on (a) 13 February and (b) 2 March 1990 at CRREL field site in Vermont (SOROIDS). There were 3 white panels and 2 metallic-coated panels in the scene on 13 Feb and 4 white panels and 1 metallic-coated panel in the scene on 2 Mar. The illuminance on a horizontal plane 15 cm above the snow cover is 15,064 lux (1400 foot-candles) on 13 Feb and 43,040 lux (4000 ft-candles) on 2 Mar. The incident solar radiation (averaged over the preceding 30 minutes) was 159 W/m² on 13 Feb and 379 W/m² on 2 Mar.

observer (Peck 1989, Pinson 1985, Houghton 1985, McCartney 1976). An object's inherent contrast is $C_o = (B_o - B_o')/B_o'$, where B_o is the brightness of the object and B_o' is the brightness of the object's immediate background.

Brightness is a term that conveys a qualitative understanding of an object's appearance. A more commonly used term to quantify the light incident at a location is luminance, which is the luminous (light) intensity per unit area normal to the direction of view. Luminous intensity at the observer's location is the light energy incident per unit time per unit solid angle from the source location. If the light originates in reflection from a surface, then the surface's luminance depends both on the nature of the illuminating radiation and on its own reflective properties. When an object and its background (both nonemitting) are illuminated similarly, their visual contrast arises from differences in the light reflected from each in the direction of the observer.

A second factor influencing visual contrast is the difference in color between the object and its background, but this is generally less significant, particularly if the color contrast is deliberately reduced in order to conceal the object.

Contrast transmission

The loss of visual contrast over the path between an object and an observer is expressed simply as

$$C_\delta = C_o \exp(-\kappa_e \delta)$$

where C_o is the inherent contrast of the object with its background at the object's location; C_δ is the apparent contrast at range δ, and κ_e is the extinction coefficient for the condition of the atmosphere and includes both absorption and scattering of light into and out of the field of view of the observer (Peck 1989). Such a representation of the loss of visual contrast encompasses two of the three causes of image degradation, namely contrast degradation due to atmospheric background radiation and forward scattering of light toward the observer by airborne particles (Kopeika 1987). The third phenomenon is turbulence, which arises from random changes in air temperature and humidity (and, less significantly, pressure) that vary air density along the propagation path; it causes the atmospheric refractive index to fluctuate randomly. The actual propagation path of the light reflected at the object is thus variable, arriving at the observer at changing angles and resulting in blurring of the image. Changes in the severity of these types of image degradation as functions of wind speed, air temperature, and relative humidity have been determined for propagation paths of several kilometers (Kopeika et al. 1986, 1990).

In physical security applications, the greatest distance an observer or camera views is typically less than a few hundred meters. Consequently, under clear sky and nonturbulent conditions, being able to resolve a camouflaged intruder visually is primarily dependent on his inherent contrast with his background. When scatterers such as falling snow, rain drops, or fog particles are present, as well as when conditions promote atmospheric turbulence, then image degradation is a factor in determining if an intruder is visible against a snow cover.

Contrast threshold

The discussion to this point has implicitly assumed that if there is visual contrast between an object and its background, and if that image is not degraded as light propagates from the object to an observer, then the observer will distinguish the object. Whether the object is seen actually depends on the threshold of contrast perception, ε, of the observer. ε is the minimum contrast detectable by the eye. Houghton (1985, p. 356) cites Blackwell's (1946) data on ε and concludes that "for values of the luminance in the typical daylight range, values of ε for a probability of detection of one-half range from 0.007 to 0.04, depending largely on the angular dimensions of the object." McCartney (1976) notes that the contrast threshold does not vary greatly, provided the background luminance is greater than 1 cd/m^2 and the object subtends an angle greater than 1°. (Unit of luminance is candela per unit area.) Therefore, ambient illumination, an intruder's size, and the contrast threshold of the observer all combine to determine whether the intruder's apparent contrast with a snow background is perceptible to the observer.

Even an intruder whose visible contrast with a snow background is below the perception level of an observer may be noticed because of shadows he casts or because his profile interrupts regular features of the scene. Visual contrast may be enhanced by reducing the amount of scattered light incident at the observer's eye or the camera's detector. A minus blue (yellow) filter will enhance visible contrast against snow on both bright and cloudy days and will especially be beneficial on cloudy days.

VISUAL CONCEALMENT AGAINST A SNOW BACKGROUND

Two examples illustrate the difficulty of successfully selecting a material to attain low visual contrast with a snow cover. Although long-term changes in snow albedo alter visual and near-infrared contrast through changes in the brightness of the snow background, variation in contrast because of change in solar illumination is more rapid and more erratic.

During a series of intrusions against two video motion detection systems at SOROIDS in 1990, Army Special Forces soldiers used an assortment of white panels to construct a visual barrier behind which they crawled. Later that winter, sections of two of the barriers (5-cm-thick styrofoam board and white-stained wall paneling) were positioned in the field of view of an east-looking black-and-white surveillance camera. Photographs and video records of the relative visual contrasts of the styrofoam and paneling with the snow cover were taken every half hour during the afternoon on 11 days in February and March.

The visual contrasts of the styrofoam and white paneling were variously zero (below perception level), positive (brighter than the background), or negative (less bright than the background). There was no consistency to which one best met the objective of having negligible visual contrast with the snow background. The visual contrasts of the styrofoam and paneling were most variable on days with intermittent cloud cover. On overcast days, the styrofoam and paneling were visually indistinguishable from the snow cover about 50% of the time, and on sunny days they were always either too bright or too dull.

The spectral reflectance of two white fabrics intended for camouflage against a snow cover are shown in Figure 2.* Reflectance measurements were made under diffuse illumination from an ultraviolet-enhanced daylight simulator. The spectrophotometer had an integrating sphere and an 8° viewing geometry. The peak reflectance at 0.44 μm is due to the fluorescent whitening agent that is added to the fabric. The reflectances are largely independent of wavelength beyond 0.5 μm. The luminances of these fabrics would perhaps be a

reasonable match to that of snow at visible wavelengths. However, the reflection of near-infrared radiation by snow is both lower and more variable with changing snow grain size and changing solar illumination characteristics (sun angle, diffuse component) than is snow's reflection of visual radiation (Appendix B). Consequently, the fabrics may provide inadequate visual concealment from a person monitoring imagery from a camera with near-infrared sensitivity.

The variability in midwinter incident solar radiation at a northern New England site such as SOROIDS is indicated by Figure 3. There are completely sunny days (25 Jan, 1 Feb, 2 Feb 1991) when the insolation is dependent on the sun angle (equivalently, time of day) and exceeds 400 W/m² for much of the daylight period. There are overcast days marked by consistently low insolation (23 Jan) or moderate variability in insolation (30 Jan). Finally, there are days with intermittent cloud cover that are characterized by large changes in insolation—between that typical of sunny days at
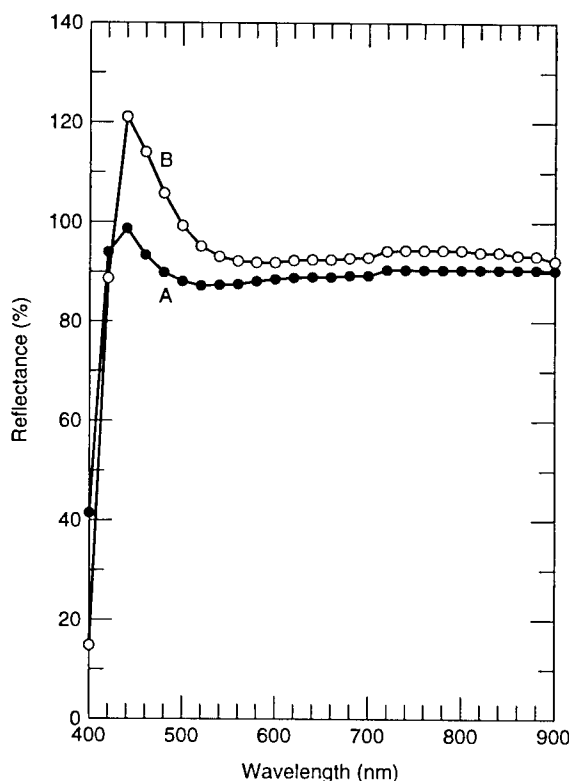

Figure 2. Spectral reflectance of two white fabrics. Fabric A is a 50/50 nylon-filled cotton oxford cloth. Fabric B is a 100% nylon, plain weave cloth.

4
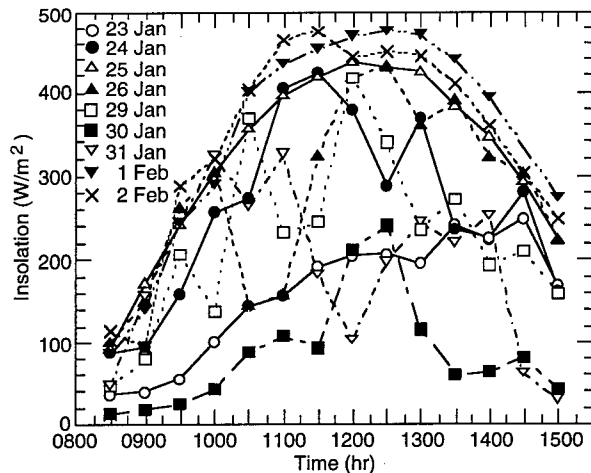
Figure 3. Incident solar radiation at SOROIDS for selected days in January and February 1991.

the optical properties of the snow surface, there may be certain sun–observer geometries for which the surface is highly reflective, such that the amount of light incident at the observer saturates his eye (or a camera's detector).

Snow-cover albedo is relevant in considerations of visual and near-infrared contrast because it indicates the relative brightness of the background compared with the level of solar illumination. It also is a factor in the luminance of the air volume within the cone of vision defined by the observer and the object. The more reflected light entering the cone of vision, the greater the potential reduction in contrast.

this time of year and levels that are significantly lower—over consecutive half-hour periods (24 Jan, 26 Jan, 29 Jan, 31 Jan). The associated snow albedos are those for predominantly direct-beam illumination, predominantly diffuse radiation, and a mixture of illumination types, respectively.

REPRESENTATIONS OF LIGHT REFLECTED FROM A SNOW COVER

The albedo of a material is the total amount of radiation reflected by the material divided by the total amount of radiation illuminating the material. For a snow cover, albedo is the ratio of reflected solar radiation to incident solar radiation, where the radiation is integrated over the entire hemisphere of possible incidence and reflection angles. If the albedo is given as a function of the wavelength of the illumination radiation, rather than for the entire solar spectrum, it is referred to as the spectral albedo of the snow cover.

The albedo of a snow cover conveys no information on the angular dependence of the amount of solar radiation reflected by a snow cover. Such information is conveyed by a bidirectional reflectance distribution function (BRDF), which is the angular distribution of reflected radiance as a function of solar incidence angle. Perovich (1994) cites previous studies of BRDF for snow and ice and presents spectral measurements of albedo and BRDF for dry snow, dry snow with a glazed surface, and other sea ice surfaces. Depending on

FIELD MEASUREMENTS DEMONSTRATING SHORT-TERM ALBEDO VARIABILITY

Changes in snow albedo due to physical changes in the snow cover occur on many time scales. There are instances of diurnal hysteresis of snow albedo, evident as albedo in the morning being higher than in the afternoon for the same solar elevation, with the pattern repeating on 24-hour cycles, which McGuffie and Henderson-Sellers (1985) attribute to a cycle of hoarfrost deposition and melting. Sublimation of hoarfrost onto the snow surface during the cold evenings and removal during the warmer daylight hours could account for the snow surface having different optical properties in the morning and afternoon. Similarly, because of grain enlargement and melting, there is a progressive decrease in albedo at a rate that can be estimated from the daily maximum temperature index, but there are also daily and hourly fluctuations about this long-term trend that are largely dependent on the level of solar radiation (Winther 1993).

Albedo of SOROIDS snow cover

Examples of snow albedo at SOROIDS indicate the diurnal variability in albedo as well as the changes in albedo over a two-week period due to aging and to fresh snowfall. The albedo of the SOROIDS snow cover is calculated from the incident and reflected solar (0.3–3 μm) radiation measured with upward- and downward-viewing pyranometers, respectively (Appendix C). Each instrument's output voltage is sampled approximately every 30 seconds by a data logger, which then averages the voltage readings over 30 minutes and reports the equivalent radiation flux per

5

unit area (in W/m^2) to a computer every half hour. The value of averaged reflected radiation is divided by the value of averaged incident radiation to obtain a snow albedo for the full 0.3-3-μm spectrum. The albedos reported here are limited to the period 0830–1500 each day because of terrain restrictions on the solar radiation incident at the site. This corresponds to sun angles between approximately 10 and 30° (Fig. A8).

Description of snow cover

The SOROIDS snow cover during this two-week period was shallow, 15 to 26 cm deep. On 23 Jan 1991 there was a 1-cm-thick crust overlying a 14-cm-deep layer of loose, rounded, elongate grains. Snow in the lower layer had a density of 0.24 g/cm^3. The most recent precipitation had been snow, sleet, and rain on 16 Jan, followed by rain on 17 Jan. A snowstorm on 28 Jan left 3–3.5 cm of fresh snow (density 0.08 g/cm^3) that began melting shortly after deposition. By 29 Jan the snow cover depth was reduced to 17 cm. A storm during the night of 30–31 Jan deposited 12 cm of snow, bringing the maximum depth of the snow cover to 26 cm on 31 Jan; the new snow was a loose, dry powder of 1 mm size angular grains and density of 0.1 g/cm^3. By the next day the new snow had compacted to a 5- to 8-cm-thick layer of loose, dry powder of density 0.15 g/cm^3; maximum snow depth now was 23 cm.

The snow cover was never deep enough that the possibility of absorption and reflection of solar radiation at the ground surface can be ignored. Evidence that the radiation penetrated the snow cover to the ground is a mid-afternoon rise in temperature at the soil surface/base of the grass cover as measured with a thermocouple (Fig. C2). Radiation absorbed at the base of the snow cover is no longer available to be returned to the downward-viewing pyranometer, so albedos will be lower than they are in the absence of absorption by the substrate.

The apparent surface temperature of the snow cover for the period 0830–1500 each day is shown in Figure 4. The temperature is calculated from the longwave (3–50 μm) radiation directed upward from the snow surface. The radiation is measured with a downward-viewing pyrgeometer and recorded as 30-min averages. The equation used to convert radiation (W/m^2) to temperature (°C) is a linear regression fit to Planck's equation with the assumptions of "black body" emission by the snow and flat, 100% response over the 3–50-μm
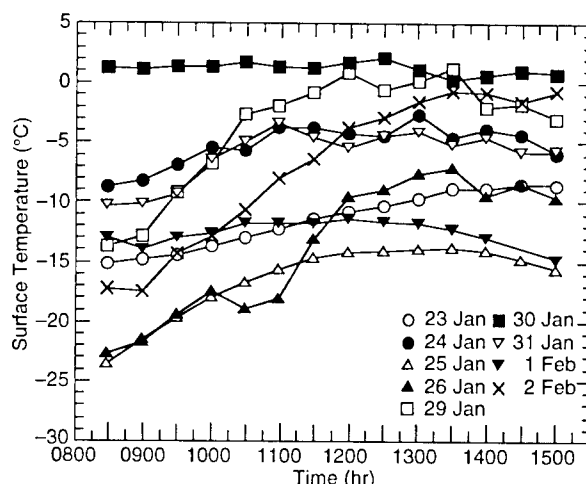

Figure 4. *Apparent surface temperature of SOROIDS snow cover on selected days in January and February 1991.*

spectrum.* The error in calculated surface temperatures is estimated not to exceed 3°C based upon the pyrgeometer response and the derivation of the equation used. The range in surface temperatures among the days results from differences in both the solar radiation available locally to warm the snow and regional weather conditions such as the temperature of air masses in contact with the snow. That is why the temperature of the snow surface is not necessarily highest on the sunniest days.

Variation with sun angle, radiation, and snow wetness

The albedos during all nine days under consideration are plotted in Figure 5 versus the time of day that the incident and reflected radiation were recorded. Taken together, the albedos define a band of values that decreases during morning hours, which correspond to increasing sun angles, is fairly independent of sun angle from 1100–1400 hr, and begins to increase in the late afternoon at successively lower sun angles. Exceptions to this are the low albedos during the morning (0830–1000) of 26 Jan and the noticeably high albedos at 1100 and 1130 on 29 Jan. For a given sun angle (refer to Fig. A8), the morning albedo generally is higher than the afternoon albedo. No observations of the snow surface are available, so it is not known
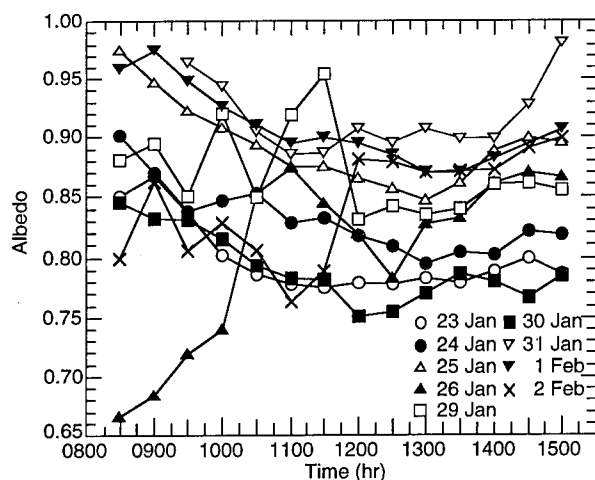
6

Figure 5. Time series records (0830–1500 hr) of snow albedo at SOROIDS on selected days in January and February 1991.

if a change in surface characteristics, such as proposed by McGuffie and Henderson-Sellers (1985), occurred between morning and afternoon on these days. Anomalies have been observed in solar radiation measurements made at the same sun angle before and after solar noon, but they are not well understood because of the large number of changes in atmospheric properties that may cause them.[*] If the solar radiation incident at the SOROIDS snow cover were relatively depleted in visible radiation in the afternoon, that could account for the lower snow albedos.

The variation in albedo with the magnitude of the incident radiation is shown in Figure 6. On these winter days the high insolation periods are ones of predominantly direct radiation.

The only day during which the snow surface was consistently at or near melting was 30 Jan (Fig. 4). The positive apparent temperature is an indication of the error inherent in the manner of calculating the surface temperature. It is probable that the near-surface portion of the snow cover was warm enough to melt on this day. With the exception of the early morning low albedo on 26 Jan, the albedo on 30 Jan was among the lowest measured (0.75–0.85). Similarly, the snow surface on 29 Jan was warm during the period 1130–1330; the pronounced drop in albedo on this day occurs between 1130 and 1200. According to the Wiscombe–

Warren model (Appendix C), an effective grain size that is large because of clustering of the wet snow grains would account for the relatively low albedo on these two days. Another factor in the decrease in albedo between 1130 and 1200 on 29 Jan is the onset (between 1100 and 1200) of a warming trend in the temperature of the near-surface soil (Fig. C2).

15-cm-deep snow cover

Considering first the 15-cm-deep snow cover of 23–26 Jan, the albedo is in the range 0.77–0.80 for most of the overcast day (23 Jan), it is in the range 0.85–0.95 during the sunny day (25 Jan), and it ranges from 0.77–0.9 on the days with intermittent cloud cover (24, 26 Jan—ignoring the early morning low albedos on 26 Jan). The trend of decreasing albedo with increasing insolation on 25 Jan is equivalent to an inverse dependence of albedo on sun angle, since the insolation on that sunny day consistently increased during the morning and decreased during the afternoon. The trend of decreasing albedo through the morning and increasing albedo through the afternoon is in agreement with the prediction of the Wiscombe–Warren model that direct beam albedo decreases as the sun angle increases.

Compared with the albedo on sunny 25 Jan, the albedo under diffuse illumination (23 Jan) is lower in the morning, which is consistent with the Wiscombe–Warren model predictions for albedo at low sun angles. Contrary to model predictions, however, the albedo under the more diffuse conditions is not higher at high sun angles. Instead, the albedo on overcast 23 Jan is low throughout the day relative to sunny 25 Jan.

The snow surface was –5°C or colder on these days, so there would have been no increase in the effective grain size due to increased wetness of the snow during melting. Consequently, change in albedo with change in grain size cannot be assessed from the data.

Although the amount of incident solar radiation was not highest on 26 Jan, the near-surface soil (beneath the snow cover, at the base of the grass cover) underwent the largest change in temperature, 1.3°C, on that day. This occurred over a diurnal cycle of predawn cooling, then late morning stabilization of temperature and afternoon temperature rise due to solar warming, and finally early evening stabilization of temperature and nighttime cooling when solar warming had ceased (Fig. C2). A thermal lag relative to the insolation cycle is evident. The strong absorption of solar

---

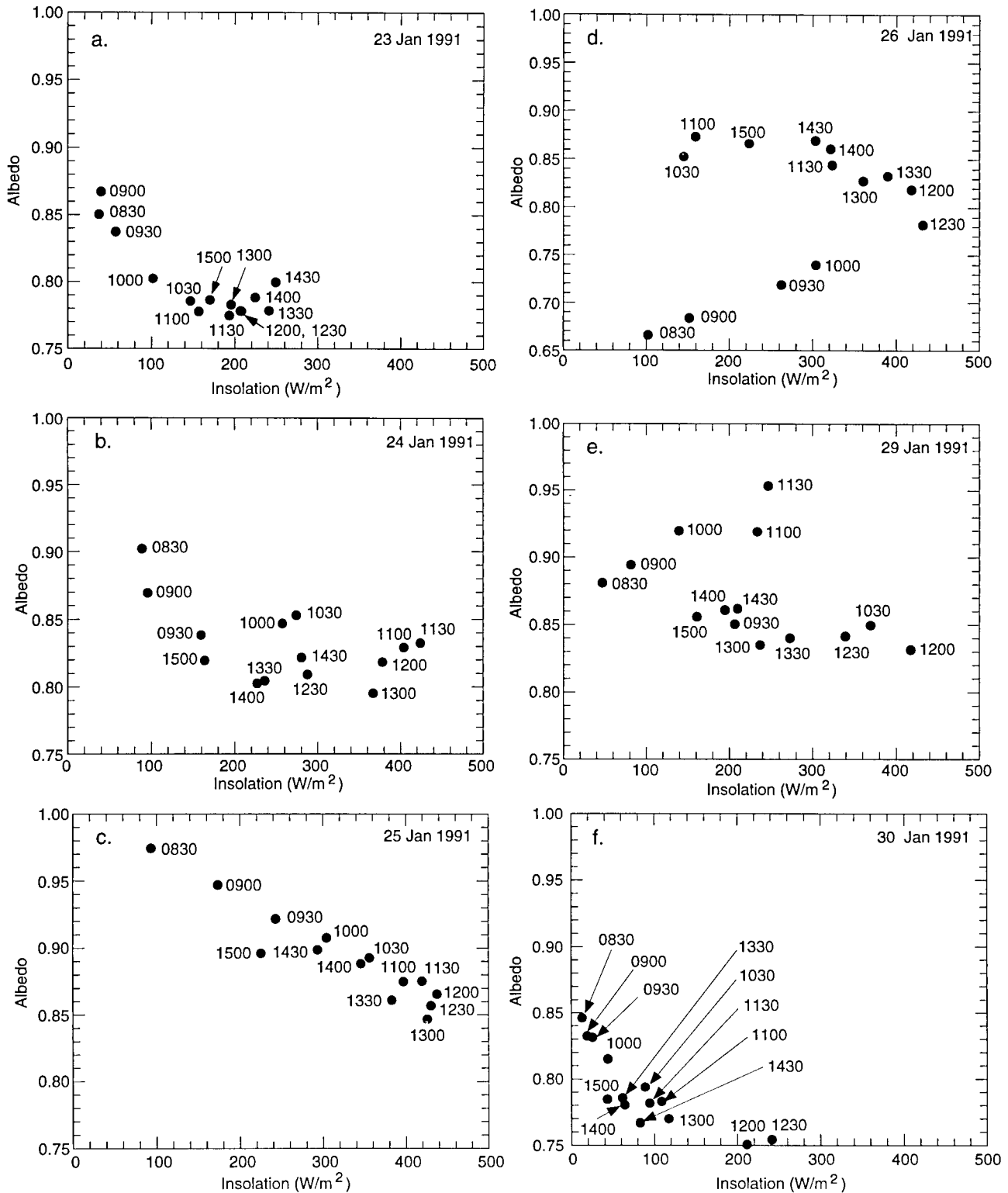[*] A. Hogan, 1994, USA Cold Regions Research and Engineering Laboratory, personal communication.

Figure 6. SOROIDS snow albedo as a function of insolation on selected days in January and February 1991.
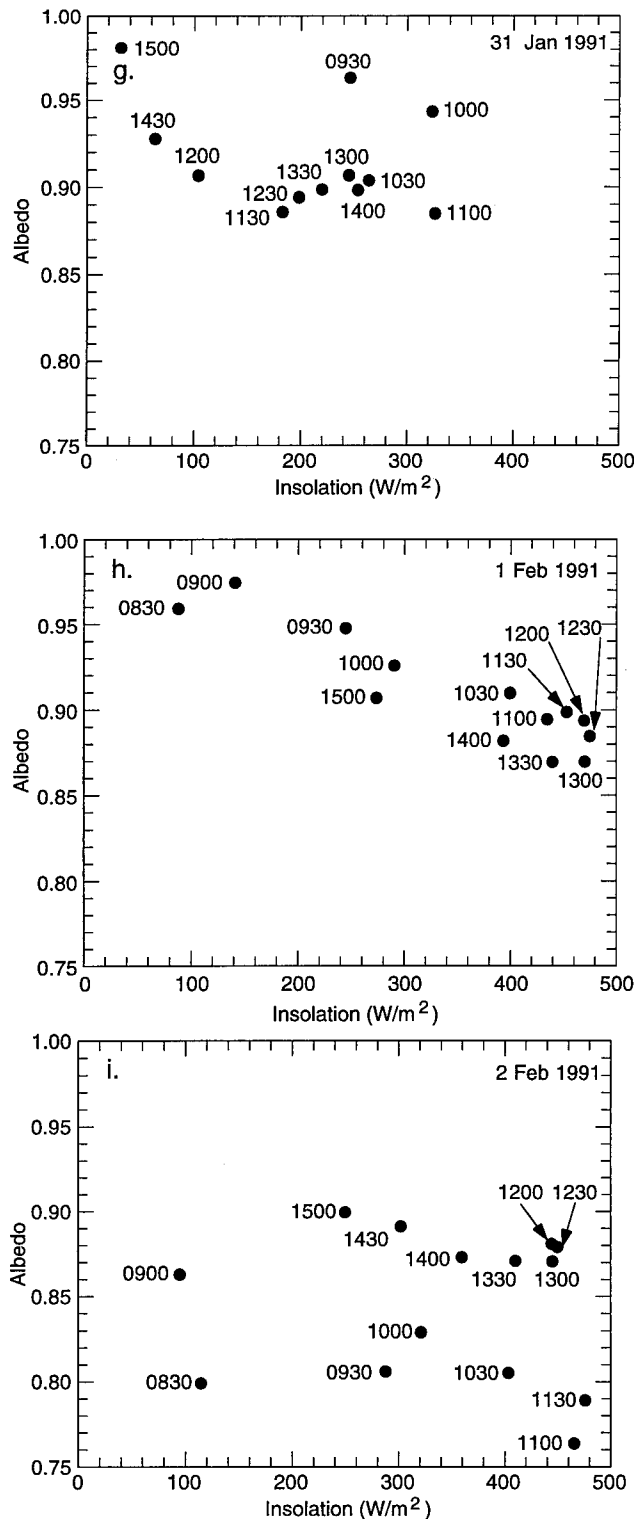
radiation that must have been occurring between 0800 and 1000 hr is a factor in the low snow albedos during that period.

23- to 26-cm-deep snow cover

The deepest snow conditions were on 31 Jan through 2 Feb. On two of these days (31 Jan, 1 Feb) there was no solar warming of the soil beneath the snow cover, at the base of the grass cover, and those were days of the highest snow albedo. The range of albedo on one sunny day (1 Feb) is 0.87–0.98 and shows a decreasing trend with increasing sun angle. On the other sunny day (2 Feb), the same trend is apparent, but less pronounced. In the morning on 2 Feb the albedo shows an overall decrease while ranging from 0.86 to 0.76, and in the afternoon it increases from 0.87 to 0.90. A damped diurnal cycle of temperature change of the near-surface soil is evident in Figure C2 for this day. Relative to 31 Jan and 1 Feb, the snow on 2 Feb was more transparent to the solar radiation, and the apparent snow albedo is expected to be less, due to the absorption of solar radiation by the soil, as is observed.

There may be a snow depth effect evident in that on 1 Feb the albedo is most often higher than it was on 25 Jan at the same time. A time-by-time comparison of the albedos on 31 Jan and 1 Feb shows that the snow albedo is relatively high under diffuse illumination (31 Jan) at high sun angles, but is not relatively low at low sun angles.

Summary of variation in SOROIDS snow albedo

During a two-week period typical of northern New England winter weather, the albedo of this shallow (15- to 26-cm-deep) snow cover is quite variable. Most values fall within the range 0.75 to 0.98. The most consistent change in albedo follows a diurnal cycle of decreasing albedo as the sun angle increases during the morning and increasing albedo as the sun angle decreases in the afternoon. Absorption of solar radiation by the soil beneath the snow cover is evident as an increase in soil temperature and is associated with lower snow albedos. This variation in the amount of light reflected from the snow cover would have caused a similar fluctuation in the visual and near-infrared contrast of an object against the snow cover.

Between snowfalls at SOROIDS there was no overall trend of decreasing albedo, such as Robinson and Kukla (1984) found occurring with snow overlying pasture land with short (<10 cm)

Figure 6 (cont'd).

9

grass and few trees (<5% of the area). Their radiation measurements were 2-min averages (made usually within 1 hour of noon) during overflights occurring every 4 days as the fresh snow cover, initially 30–55 cm deep, aged. Daily maximum air temperatures were above freezing (4–11°C) and there was no significant rain or snowfall during this period. The albedo decreased from 0.72 on 14 Feb to ~0.64 on 18 Feb, and eventually to ~0.33 on 1 Mar 1983. In contrast, at SOROIDS the daily maximum air temperature at a height of 2 m was above freezing only on 29 Jan (5°C), 30 Jan (4°C), and 2 Feb (7°C), and the snow surface warmed to 0°C for extended periods only on these three days. The enlargement of snow grains that likely accompanied the warmer conditions of the Robinson and Kukla study may well account for their trend of decreasing albedo.

DESIGNING FIELD TRIALS OF VISUAL DETECTION WITH A SNOW BACKGROUND

Based on the examples presented of 1) variability in visual contrast of white objects against a snow cover and 2) variability in albedo of a northern New England snow cover, the following recommendations are made.

Field determinations of visual contrast with a snow background, either to assess the effectiveness of a camouflage material or to test the detection capability of a video motion detection system, should include sunny and overcast days. On intermittently overcast days, it is necessary to monitor the incident solar radiation so that the visual contrast results may be categorized as pertaining to direct or diffuse illumination. Even on apparently clear-sky days there may be changes in the solar radiation incident at the ground that would be detected by a pyranometer but probably be unnoticed by observers characterizing the sky condition. Atmospheric turbidities comparable to those associated with clouds are frequently observed in apparently clear air. These are associated with density gradients and subvisible droplets formed in rising air masses where no visible cloud is formed.*

There should be frequent trials during the morning or afternoon in order to span the range of

_____

*A. Hogan, 1994, USA Cold Regions Research and Engineering Laboratory, personal communication.

albedos associated with the diurnal variation in solar elevation. The Wiscombe–Warren model quantifies the dependence of snow albedo on sun angle for a flat snow surface. If the snow surface is rough (has noticeable undulations or other relief), then the light reflected from the snow may depend on the orientation of these surface features to the incident solar radiation.

The trials preferably should be conducted early or late in the winter when maximum potential insolation and maximum sun angle are greatest. A disadvantage of this scheduling is that midwinter snow covers generally are deeper.

Snow cover properties (grain size, wetness, and depth) should be documented so that the variation in albedo due to changing grain size (actual or effective) and relative absorption of solar radiation by the ground cover may be considered when assessing the trial results.

The surface temperature of the ground or pavement beneath the snow cover should be monitored so that the relative loss of solar radiation through absorption by the substrate (and consequent decrease in apparent snow albedo) can be assessed.

SUMMARY

Daily and longer-term variation in snow albedo affects all areas of physical security that involve visual or near-infrared contrast with a snow cover. As the amount of natural light reflected by a snow-covered background changes, an intruder becomes more or less detectable through direct observation, by viewing a camera scene, or with a video motion detection system.

An example of the magnitude and rate of change in snow albedo is given for a shallow (15- to 26-cm-deep) snow cover at a northern New England site. The albedo mostly varied from 0.75 to 0.98 over a two-week period, 23 Jan–2 Feb 1991. The most consistent variation was a decrease in albedo during the morning as the sun angle increased and a corresponding increase in albedo with decreasing sun angle in the afternoon. The albedo was low when the snow surface temperature indicated melting was occurring or when an increase in temperature of the soil beneath the snow cover indicated solar radiation was being absorbed by the soil.

The potential variation in visual and near-infrared contrast of a white object with a snow background can be estimated from the reflective properties of the object together with model predic-

10

tions of snow albedo as a function of grain size, solar elevation, and ratio of diffuse to direct solar radiation. The diurnal variation in sun angle and the seasonal variation in maximum potential solar radiation at a site can be calculated from site latitude and longitude and calendar date, modified by site terrain that influences day length.

LITERATURE CITED

Blackwell, H.R. (1946) Contrast thresholds of the human eye. *Journal of the Optical Society of America,* **36:** 624–643.

Coulson, K.L. (1975) *Solar and Terrestrial Radiation, Methods and Measurements.* New York: Academic Press.

Dozier, J. (1989) Remote sensing of snow in visible and nearinfrared wavelengths. In *Theory and Applications of Optical Remote Sensing* (G. Asrar, Ed.). New York: John Wiley, pp. 527–547.

Erbs, D.G., S.A. Klein and J.A. Duffie (1982) Estimation of the diffuse radiation fraction for hourly, daily and monthly average global radiation. *Solar Energy,* **28:** 293–302.

Gerdel, R.W., M. Diamond, and K.J. Walsh (1954) Nomographs for computation of radiation heat supply. SIPRE Research Paper 8. Available from USA Cold Regions Research and Engineering Laboratory.

Halliday, D. and R. Resnick (1974) *Fundamentals of Physics.* New York: John Wiley and Sons.

Grenfell, T.C. and D.K Perovich (1981) Radiation absorption coefficients of polycrystalline ice from 400–1400 nm. *Journal of Geophysical Research,* **86:** 7447–7450.

Houghton, H.G. (1985) *Physical Meteorology.* Cambridge, Mass.: MIT Press.

Kierkus, W.T. and W.G. Colborne (1989) Diffuse solar radiation daily and monthly values as affected by snow cover. *Solar Energy,* **42:** 143–147.

Kopeika, N.S. (1987) Imaging through the atmosphere for airborne reconnaissance. *Optical Engineering,* **26:** 1146–1154.

Kopeika, N.S., A.N. Seidman, I. Dinstein, C. Tarnasha, R. Amir and Y. Biton (1986) How weather affects seeing through the atmosphere. *Optical Engineering,* **25:** 505–512.

Kopeika, N.S., I. Kogan, R. Israeli and I. Dinstein (1990) Prediction of image propagation quality through the atmosphere: The dependence of atmospheric modulation transfer function on weather. *Optical Engineering,* **29:** 1427–1438.

McCartney, E.J. (1976) *Optics of the Atmosphere.* New York: John Wiley and Sons.

McGuffie, K. and A. Henderson-Sellers (1985) The diurnal hysteresis of snow albedo. *Journal of Glaciology,* **31:** 188–189.

Mecherikunnel, A.T., J.A. Gatlin, and J.C. Richmond (1983) Data on total and spectral solar irradiance. *Applied Optics,* **22:** 1354–1359.

Peck, L. (1989) Contrast and visibility under winter conditions with application to motion detection systems. USA Cold Regions Research and Engineering Laboratory, CRREL Report 89-17.

Perovitch, D.K. (1994) Light reflected from sea ice during the onset of melt. *Journal of Geophysical Research,* **99:** 3351–3359.

Pinson, L.J. (1985) *Electro-Optics.* New York: John Wiley and Sons.

Robinson, D.A. and G. Kukla (1984) Albedo of a dissipating snow cover. *Journal of Climate and Applied Meteorology,* **23:** 1626–1634.

Rodgers, A.L., I.B.R. Fowler, T.K. Garland-Collins, J.A. Gould, D.A. James and W. Roper (1983) *Surveillance and Target Acquisition Systems.* Brassey's Battlefield Weapons Systems and Technology Volume VII. Oxford: Brassey's Defense Publishers.

Smithsonian (1984) *Smithsonian Meteorological Tables.* Smithsonian Misc. Collections, vol. 114. Washington, D.C.: Smithsonian Institution Press.

Wallen, C.C. (1948–49) Glacial-meteorological investigations on the Karsa Glacier in Swedish Lapland. *Geografiska Annaler,* 240 p.

Warren, S.G. and W.J. Wiscombe (1981) A model for the spectral albedo of snow. II: Snow containing atmospheric aerosols. *Journal of Atmospheric Sciences,* **37:** 2734–2745.

Winther, J.-G. (1993) Short- and long-term variability of snow albedo. *Nordic Hydrology,* **24:** 199–212.

Wiscombe, W.J. and S.G. Warren (1980) A model for the spectral albedo of snow. I: Pure snow. *Journal of Atmospheric Sciences,* **37:** 2712–2733.

APPENDIX A: SOLAR ILLUMINATION

Nearly all the solar radiation incident at the earth's surface is in the 0.3–2.5-μm wavelength band. The visible spectrum is generally defined as 0.43–0.69-μm wavelengths because beyond these limits the eye sensitivity has dropped to 1% of its maximum value (Halliday and Resnick 1974, Coulson 1975). Because the electronic detectors used in surveillance cameras may be sensitive to longer wavelengths, solar radiation in the wavelength band 0.4–1.2 μm is relevant to this report.

Solar radiation incident at a site varies due to many factors. As a consequence of the earth's orbit around the sun and its tilted axis of rotation, the available solar radiation depends on the time of year. The total solar radiation (kJ/m^2) falling on a horizontal surface at the top of the atmosphere during one day is shown in Figure A1 for selected days in the northern hemisphere winter (Smithsonian 1984, Table 132). This is based on a solar constant of 1353.7 W/m^2 (1.94 $cal/cm^2/min$) determined from measurements at high-altitude ground stations. The solar constant is defined as the flux of solar radiant energy across a surface of unit area oriented normal to the solar beam at the mean sun–earth distance. It varies slightly from the actual solar radiation incident at the outer limit of the atmosphere, which depends on seasonal differences in the distance between the sun and the earth.

The amount of direct (unscattered) solar radiation that propagates through the atmosphere to be incident at the ground surface depends regionally on the properties of the atmosphere. It also depends on the solar altitude because that determines the path length of the radiation through the atmosphere. Radiation is lost from the direct beam through scattering on air molecules, water droplets, and dust, through absorption by atmospheric gases and particulates, and through reflection at the top and base of clouds (Coulson 1975, Mecherikunnel et al. 1983, Houghton 1985). At near-infrared wavelengths, there are strong absorption bands caused by water vapor and minor absorption by carbon dioxide. Transmission of visible and ultraviolet radiation is strongly dependent on absorption by ozone and scattering by air molecules. Absorption and scattering by aerosols are variable and somewhat location-dependent because industrial and natural sources of aerosols are not uniformly distributed.

A representative range of values of total daily direct solar radiation incident at a horizontal surface on the ground during a northern hemisphere winter is plotted in Figure A2 for different atmospheric transmission coefficients (Smithsonian 1984, Table 135). Under cloudless sky conditions the atmospheric transmission coefficient is 0.90, which means that 90% of the solar radiation incident on a horizontal surface outside the atmosphere is actually received upon a horizontal area of the ground surface. Smaller transmission coefficients express increasingly greater attenuation due to scattering and absorption. Gerdel et al. (1954) cite Wallen's (1948–49) empirical relationship between total radiation incident at the earth's surface and mean cloudiness as showing that the decrease in radiation is small (10%, relative to clear sky radiation) when the mean cloudiness during daylight hours is 5/10, and that complete overcast (10/10) reduces the incident radiation to 50% of its clear sky value.

Diffuse sky radiation is also incident at the ground surface. One component is radiation that was scattered out of the direct beam on its passage through the atmosphere. The diffuse sky radiation reaching a horizontal surface at the ground under cloudless conditions is plotted in Figure A3 for representative atmospheric transmission conditions on selected days during the northern hemisphere winter. The diffuse radiation was calculated from the difference between the total daily radiation at the top of the atmosphere, decremented by 9% to account for water vapor absorption (7%) and ozone absorption (2%), and the total daily direct solar radiation reaching the ground. That difference approximates the total energy
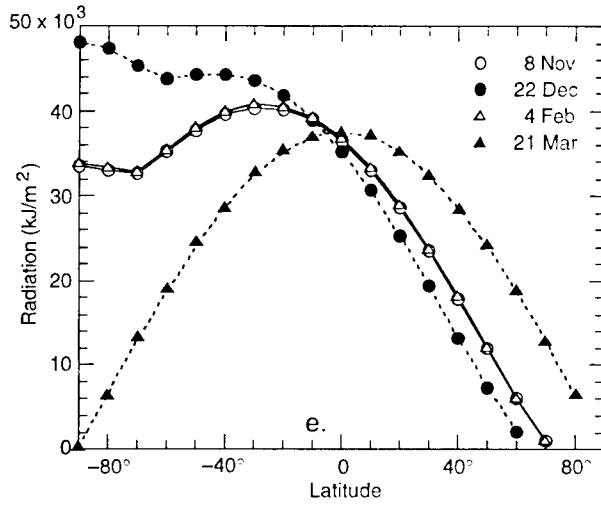
Figure A1. Total solar radiation falling on a horizontal surface at the top of the atmosphere during one day (from Smithsonian 1984, Table 132).
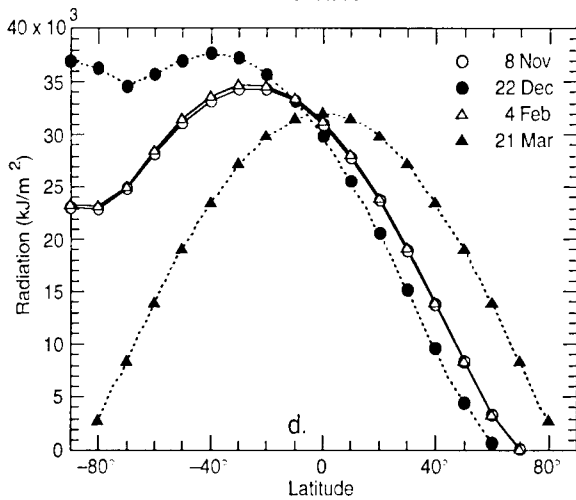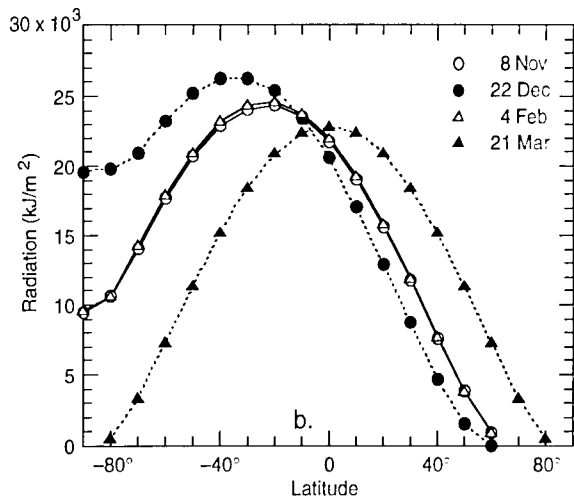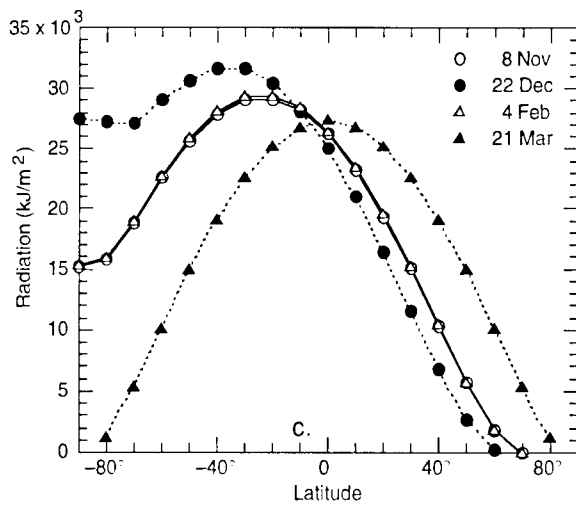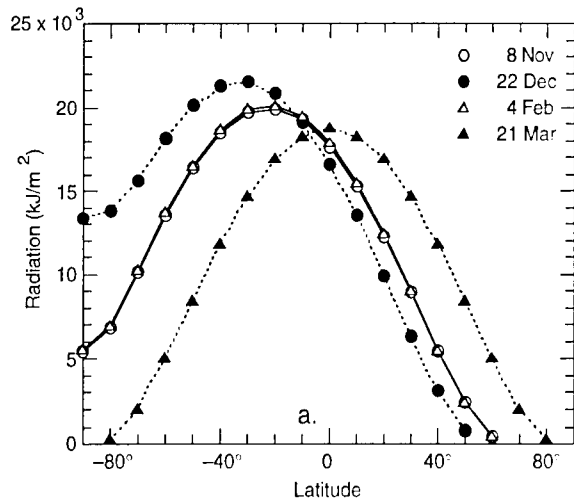

Figure A2. Total daily direct solar radiation incident on a horizontal area of the ground for atmospheric transmission coefficient = (a) 0.6, (b) 0.7, (c) 0.8, and (d) 0.9 (from Smithsonian 1984, Table 135).

14

scattered out of the solar beam. One half of that amount is the diffuse radiation incident at the ground, assuming that half the radiation is scattered forward, toward the ground, and half is scattered backward (Smithsonian 1984, p. 420). The ratio, I_d/I, of hourly diffuse radiation to hourly global (horizontal) radiation is high, ~1.0, when the hourly clearness index, k_T, the ratio of hourly global radiation to the hourly extraterrestrial radiation, does not exceed 0.3. The diffuse component of the global radiation diminishes rapidly as the atmosphere clears ($0.3 < k_T < 0.7$), and is 20% for atmospheres with higher clearness indices (Erbs et al. 1982).

A second component of diffuse radiation incident at the ground is radiation that has been reflected at cloud surfaces before reaching the ground or that has reached the ground a second time following reflections first at the ground surface and then at the base of a cloud cover. Cloud height, thickness, and coverage strongly influence this component of incident radiation. Coulson (1975) compares the intensity of diffusely transmitted light with the intensity of light reflected off a snow cover that is then backscattered toward the ground again. For a zenith sun (sun angle of 90°), the backscattered surface-reflected light off new snow is likely to be greater due to the highly reflective snow surface. The surface albedo must be ~1.0 for an equivalence between the two when the sun angle is 36.9°, while at a sun angle of 11.5° the intensity of the diffusely transmitted light is greater regardless of the snow albedo.
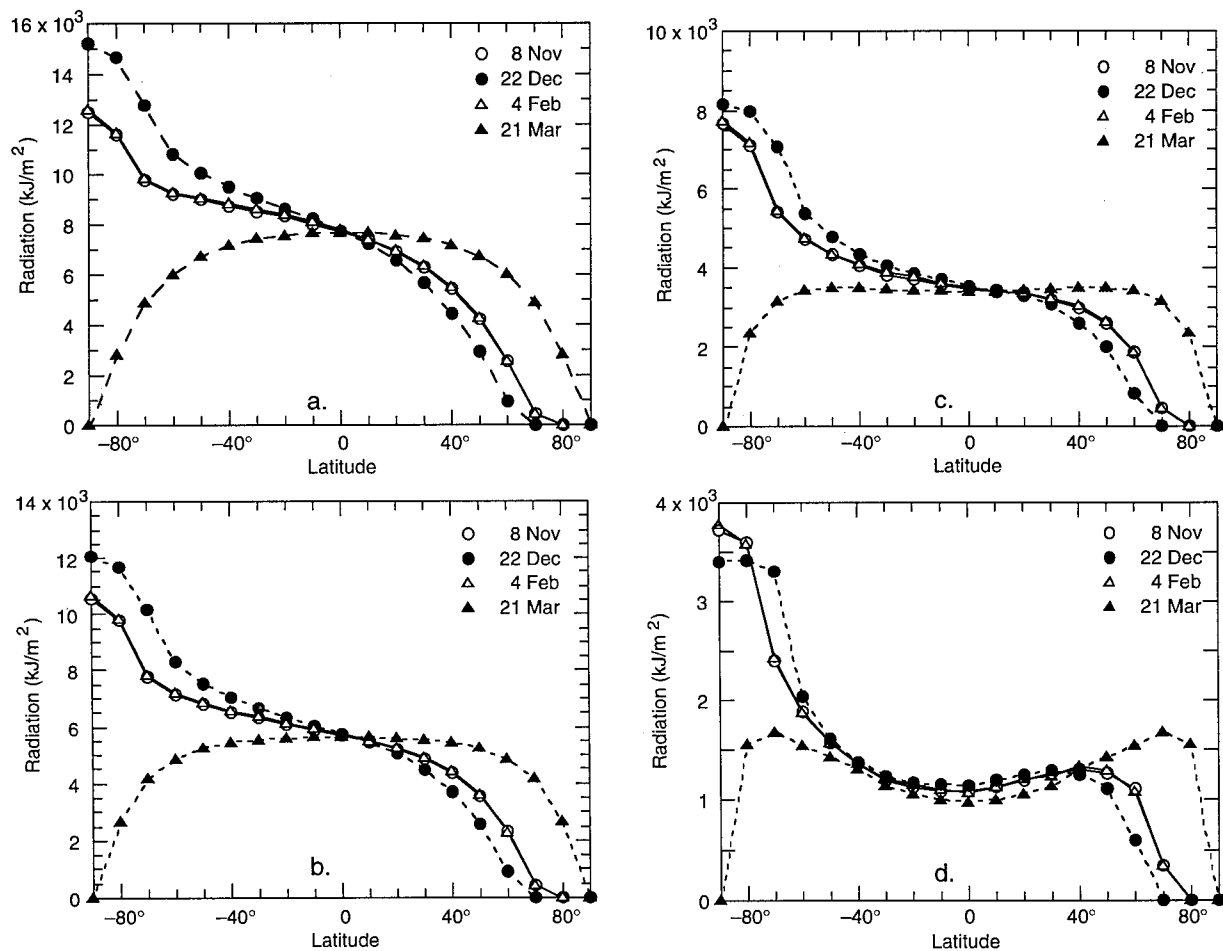

Figure A3. Total daily diffuse solar radiation incident on a horizontal area of the ground for an atmospheric transmission coefficient of (a) 0.6, (b) 0.7, (c) 0.8, and (d) 0.9.
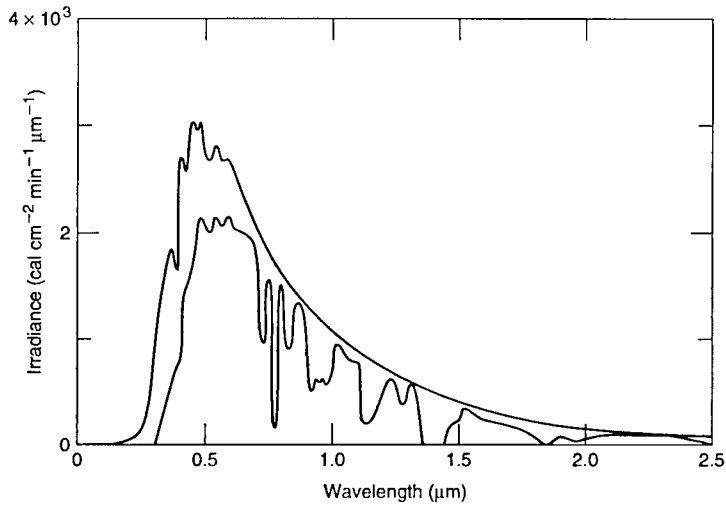
15

Figure A4. Solar spectral irradiance outside the atmosphere and at the surface of the earth (from Houghton, Fig. 3.6). The optical air mass is 2.0, the precipitable water is 1 cm, and the atmosphere is free of aerosol. (Optical air mass is the slant path through the atmosphere relative to the normal incidence path.) 1 cal/cm^2/min = 697.8 W/m^2.
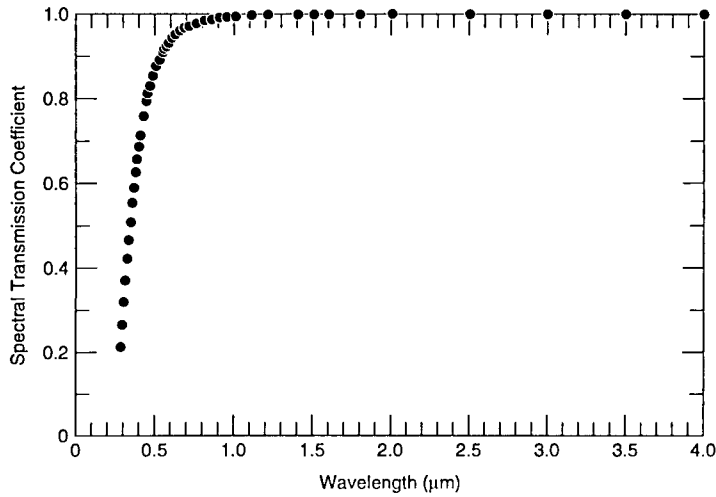

Figure A5. Spectral transmission coefficient of radiation through pure, dry air (from Smithsonian 1984, Table 144).
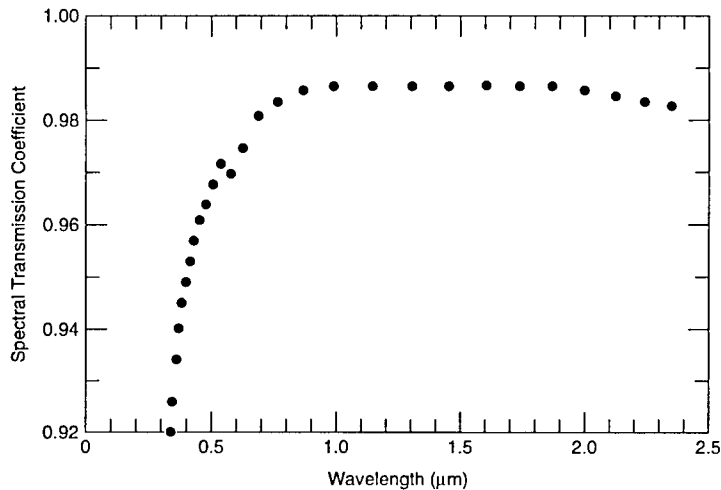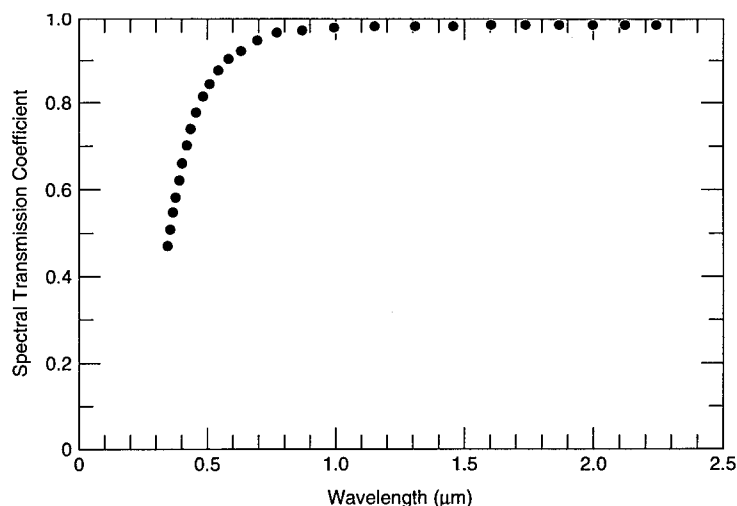

Figure A6. Spectral transmission coefficient of radiation through the atmosphere containing 1 cm of precipitable water. No other attenuation effects are considered (from Smithsonian 1984, Table 145).

Figure A7. Spectral transmission coefficient of solar radiation through a cloudless, dust-free atmosphere containing 1 cm of precipitable water.

In general, the diffuse radiation incident at the ground following at least one surface reflection will be higher when the ground is snow-covered than for other ground covers because the visible albedo of snow is high. Daily values of diffuse radiation are as much as 30–40% higher (depending on the daily atmospheric clearness index) when the ground is snow-covered (Kierkus and Colborne 1989). The diffuse light, however, will be relatively enriched at visible wavelengths because of the spectrally dependent albedo of snow.

A consequence of light being multiply reflected between the base of a cloud and the snow cover, or being multiply scattered in general, is that the scene becomes uniformly illuminated. In turn, visible contrast between the ground surface and sky is low or absent. This situation, termed overcast whiteout, is possible during bright daylight or bright moonlight. Near-infrared contrast may persist during the whiteout because the albedo of snow is lower at near-infrared wavelengths.

Except where the terrain is flat and featureless, there is likely to be a third component of diffuse radiation incident at the ground. This is atmospherically scattered radiation that subsequently reflects off buildings, hills, and other features to become directed at the ground.

The transmission of solar radiation through the atmosphere (Fig. A4) is wavelength-dependent. The transmission factor for pure, dry air is given in Figure A5 (Smithsonian 1984, Table 144). These are computed values, for the case of dust-free air and negligible absorption by permanent gases, obtained from theoretical expressions for scattering by air molecules. Transmission of visible radiation increases with wavelength. Transmission is high at the near-infrared wavelengths represented, but at other near-infrared wavelengths is strongly depleted, as Figure A4 shows. If only the effect of scattering by water vapor is considered, the transmission coefficient for radiation passing through an air column that contains 1 cm of precipitable water (if all the water vapor in the vertical air column were condensed, it would form a layer 1 cm thick) is shown in Figure A6 (Smithsonian 1984, Table 145); the measurements do not extend to ultraviolet wavelengths. For larger atmospheric water vapor contents the transmission coefficient is raised to a power w, where w is the amount of precipitable water in the path. Overall, transmission of visible radiation again increases with wavelength. The net transmission factor is the product of that for pure, dry air times that for scattering of solar radiation by water vapor. This is shown in Figure A7 for an atmosphere containing 1 cm of precipitable

17

Table A1. Times of selected sun angles on days representative of northern New England winter and transitional periods (location: 45°N, 73°W).

Angle (degrees)	22 Nov	22 Dec	21 Jan	23 Feb	21 Mar	16 Apr
0	6:58	7:35	7:23	6:46	5:54	5:12
5	7:33	8:05	7:58	7:11	6:24	5:32
10	8:08	8:45	8:33	7:41	6:49	6:02
15	8:53	9:40	9:18	8:11	7:19	6:32
20	9:38	10:45	10:03	8:56	7:49	6:57
25	10:38		11:03	9:36	8:14	7:32
30				10:11	8:54	7:52
30				14:01	15:04	15:37
25	12:18		12:43	14:36	15:29	16:02
20	13:38	12:55	14:03	15:16	16:04	16:32
15	14:23	14:10	14:48	15:51	16:34	16:57
10	15:03	14:50	15:28	16:16	16:59	17:27
5	15:38	15:35	16:03	16:51	17:29	17:52
0	16:03	16:05	16:28	17:21	17:54	18:27

water. The result of the various transmission losses is that the solar radiation reaching the ground is depleted overall at the visible wavelengths and depleted selectively at near-infrared wavelengths.

The potential angle of incidence of the direct solar beam with the ground surface varies with the latitude and the time of year in a predictable manner, whereas the actual angle of incidence is dependent on the local terrain. The local (Eastern Standard) time when the sun angle is 0, 5, 15, 20, 25, or 30° is given in Table A1 and Figure A8 for a flat, featureless site at 45° north latitude, 73° west longitude on days spanning the winter season. The sun angles were calculated using an analemma and sun chart. The variation in elevation of the sun in the sky and in the duration of daylight during the northern hemisphere winter are evident.

Other natural sources of illumination are starlight and moonlight. Figure A9, from Rodgers et al. (1983), compares their spectral content.
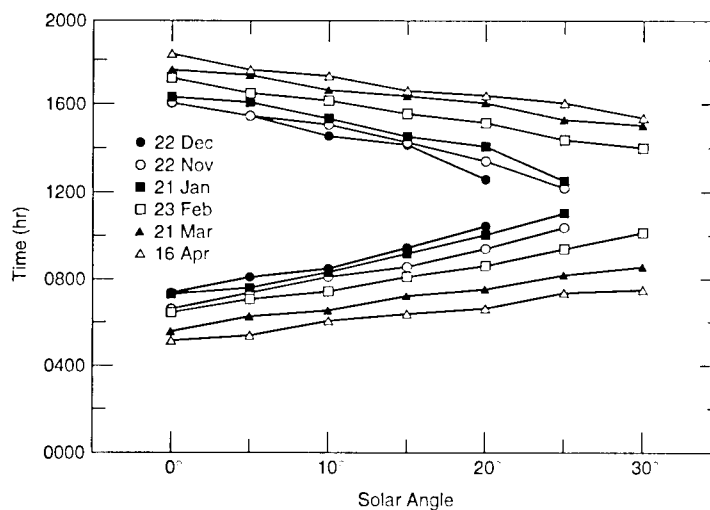
Figure A8. Times of sun angles at a 45° north latitude, 73° west longitude location. Terrain effects are neglected.
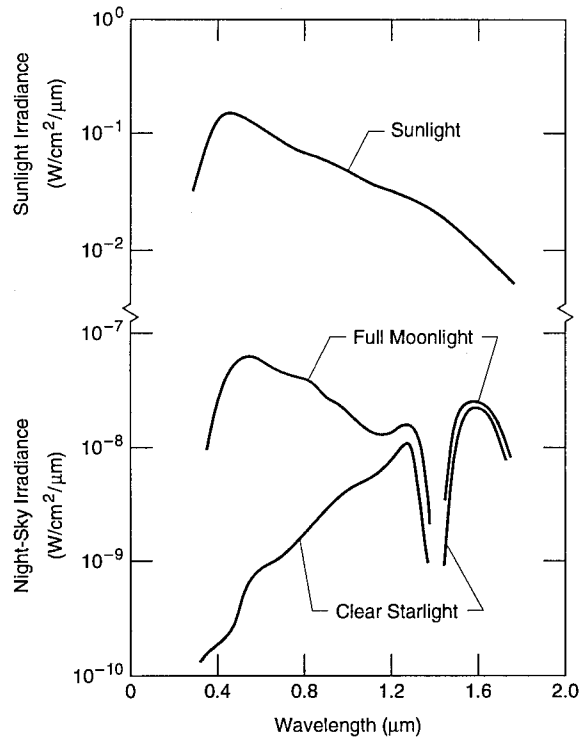
18

Figure A9. Spectral content of sunlight, moonlight, and starlight (from Rodgers et al. [1983]).

APPENDIX B: REFLECTION OF LIGHT BY A SNOW COVER

General information

Light reflected off a snow cover is the end result of a complex interaction between the incident light and the snow grains. The reflection process is actually the scattering of photons back out of the snow cover. General discussions of light scattering by particles are given in Houghton (1985) and McCartney (1976). When a photon is incident at a snow grain, internal oscillations are set up that allow each ice molecule to act as a reradiator of electromagnetic energy. (There is no net change in an ice molecule's internal energy state as there would be upon the absorption of photons.) The pattern of reradiated energy is dependent on the size of the scattering particle. Each subsequent scattering event redirects photons with little accompanying absorption until eventually an amount of light nearly equivalent to that initially incident on the snow cover re-emerges. The scattering may take place at the snow surface (surface reflections) by interaction with a single snow grain or by multiple scattering among deeper snow grains (volumetric scattering). In the context of geometric optics (Pinson 1985), the light has been refracted by the snow grains because of the different indices of refraction of air and ice. Liquid water within the snowpack does not on its own affect the snow's albedo because ice and water have closely similar indices of refraction; however, individual ice grains cluster together in the presence of water, so there is a dependence of albedo on snow wetness through this indirect grain size effect, with the albedo of snow at near-infrared wavelengths being lower in wet snow (Dozier 1989, Wiscombe and Warren 1980).

The amount of reflected visible radiation is high, varying only slightly, because ice is highly transparent at these wavelengths. Absorption in ice is both greater and more strongly a function of wavelength in the near-infrared region, so with the exception of absorption minima centered on ~1.8 and 2.25 μm, the amount of reflected radiation is much less and more spectrally variable in the near-infrared (Grenfell and Perovich 1981).

There is an extensive literature on field measurements of snow albedo. The application of this report, however, requires a general understanding of the causes and relative magnitudes of differences in the quantity of light reflected by a snow surface, which will be based on the Wiscombe–Warren model for the spectral albedo of snow. The selected model has been used to predict reflected solar radiation under all the situations relevant to this report: aging of the snow cover (grain enlargement through metamorphism), different sun angles, and clear and cloudy sky conditions.

Wiscombe–Warren model predictions

The Wiscombe and Warren model (1980) for the albedo of spherical snow grains combines multiple scattering based on a bulk radiative transfer approach (Delta–Eddington approximation), with a representation of single scattering based on Mie theory, which is applicable to particle radius/wavelength ratios on the order of 0.1–10. The model predicts the spectral albedo of snow as a function of grain size, solar elevation, and ratio of diffuse to direct incident solar radiation; if the snow cover is shallow (on the order of 20 cm or less for new or fine-grained snow) so that a portion of the incident radiation penetrates the snow to be absorbed by the ground, then snow layer thickness and the albedo of the soil (or ground cover) are additional parameters. The calculated albedo is for hemispherical reflection of radiation incident from a certain direction, i.e., the reflected radiation is summed over the entire range (0–180°) of angles at which radiation may leave the surface. This model predicts snow spectral albedos that are as much as 10% higher than the measured albedo of snow in the visible spectrum. Warren and Wiscombe (1980) consider the extent to which soot, or other impurities that are more absorptive than ice, lower the albedo of natural snow.
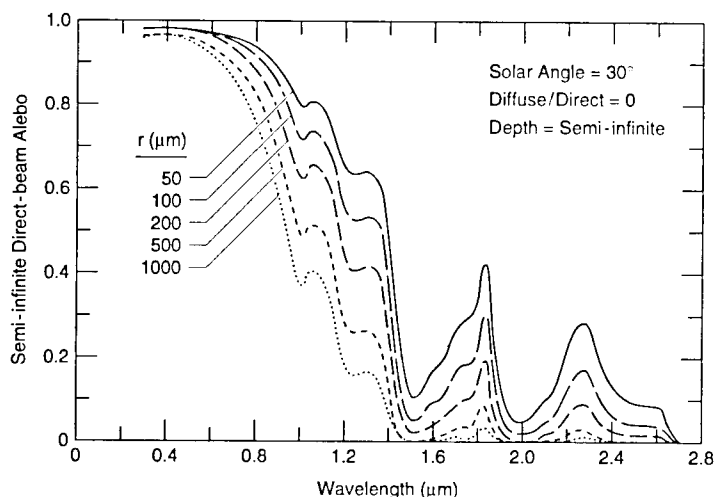
Figure B1. Wiscombe–Warren model predictions of direct-beam spectral albedo of a semi-infinite snow cover for different grain sizes (from Wiscombe and Warren 1980).

The Wiscombe–Warren model predicts that the direct-beam spectral albedo of a semi-infinite snow cover decreases as the radius of the snow grains increases (Fig. B1). They consider grain radii of 50, 200, and 1000 µm as representative of new snow (20–100 µm), fine-grained older snow (100–300 µm), and old snow near the melting point (1.0–1.5 mm), respectively. Although the decrease in direct-beam albedo at visible wavelengths is slight, from ~0.98 to 0.9, the albedo for 1.4-µm radiation drops from ~0.65 to 0.1. Since as a snow cover ages the snow grains that persist enlarge at the expense of other grains that lose mass due to vapor transport, the net result is an increase in grain size. Were no other changes to occur to the surface of the snowpack—no deposition of fresh snow, no glaze or crust formation following a melt–freeze cycle or rainfall—then under the same weather conditions the amount of light reflected from the snow surface would be less with time. Unless a com-
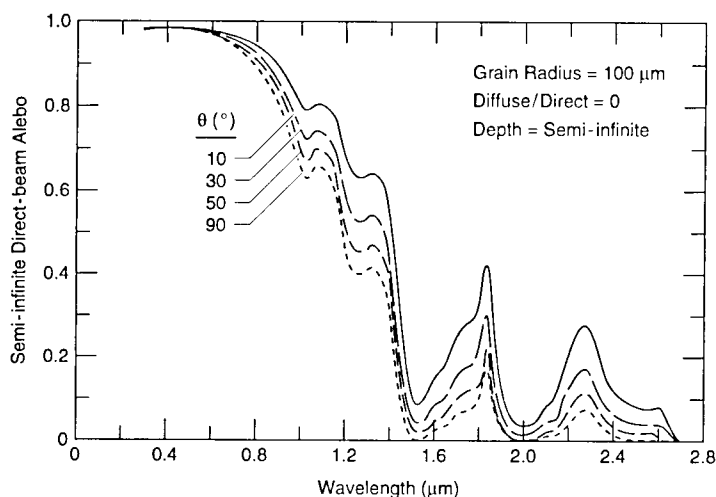

Figure B2. Wiscombe–Warren model predictions of direct-beam spectral albedo of a semi-infinite snow cover for different sun angles (from Wiscombe and Warren 1980).
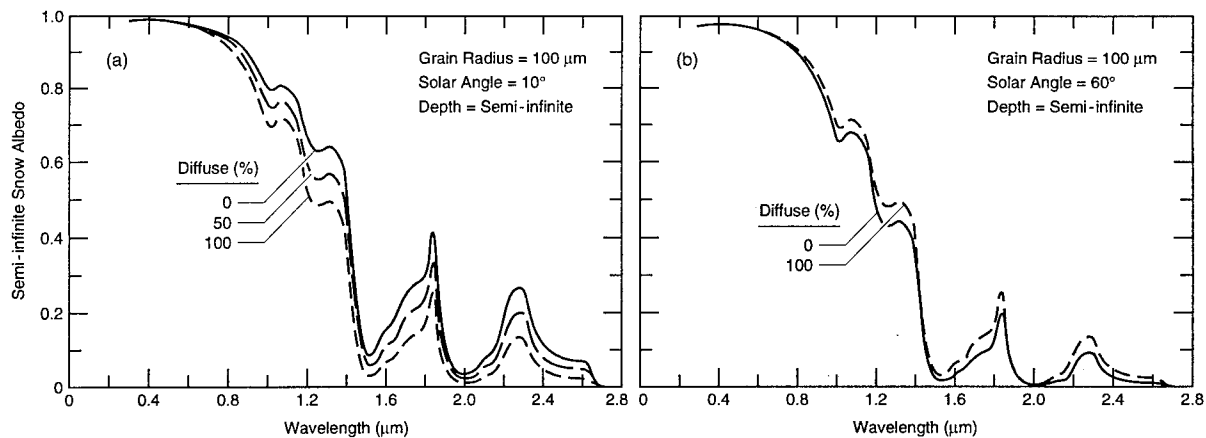
22

Figure B3. Wiscombe–Warren model predictions of spectral albedo of a semi-infinite snow cover for different ratios of diffuse to direct radiation and sun angles of (a) 10° and (b) 60° (from Wiscombe and Warren 1980).

pensating change occurred in the reflective properties of a white object in the scene, the decrease in luminance of the snow cover would alter the visual contrast of the white object.

The model also predicts that the direct-beam spectral albedo of a flat, semi-inflnite snow cover increases as the sun angle decreases (Fig. B2). The more obliquely the solar radiation is incident at the snow surface, the more intense the reflected component is. The increase is slight for visible radiation, but may be 30–40% for near-infrared radiation. Assuming that no significant physical changes are occurring to the snow cover, then from sunrise to sunset the direct-beam albedo of snow is first decreasing and then increasing as the sun angle varies. The proportion of reflected solar radiation would be highest just after sunrise and just before sunset, but the amount of incident solar radiation at those times (assuming clear sky conditions throughout the day) would be least. Both the snow cover and a white object in the scene would be receiving the least solar illumination when the direct-beam albedo of the snow cover would be the maximum of its (clear sky) diurnal variation. Any irregularity to the snow surface would impart a different angular dependence to the albedo.

Finally, considering both direct and diffuse illumination, the Wiscombe–Warren model predicts that the spectral albedo of a semi-infinite snow cover decreases at low sun angles as the percentage of diffuse illumination increases, and that the reverse is true at high sun angles (Fig. B3). The difference in albedo is large for near-infrared radiation and small for visible radiation. This can have the most dramatic effect on the visual and near-infrared contrast of a white object against the snow cover since changes in the proportions of diffuse and direct radiation can occur as rapidly as the cloud cover varies.

All of the cited changes in snow albedo, as predicted by the Wiscombe–Warren model, are most pronounced for the near-infrared wavelengths. The resultant changes in visual contrast will be more evident when viewing a scene produced by a camera with near-infrared sensitivity than when viewing the object and snow cover directly.

23

APPENDIX C: ALBEDO MEASUREMENTS AND SITE CHARACTERISTICS

The CRREL test site, known as SOROIDS, is a level portion of a 25-acre field along the White River in South Royalton, Vermont. A frequently traveled secondary road and rail line run along the western boundary of the field, and a heavily traveled state route follows the opposite side of the White River. The snow cover is exposed to all the contaminants of semirural society, including soil dust blown off the cultivated portion of the field whenever the snow is not continuous or deep enough to stabilize the exposed soil.

The radiation measurements are made with Eppley pyranometers mounted at a constant height of 1.5 m above the ground (not snow) surface. The pyranometers are attached to an aluminum lever arm that extends horizontally from a vertical aluminum support post. The lever arm and post are to the north of the pyranometers so they do not block direct sunlight. The pyranometers are calibrated by Eppley once a year. Each month the upward and downward pyranometers temporarily are rotated 180° (to reverse their direction of view) and their output is compared for consistency with each other.

A 4-m-high openwork aluminum tower to which meteorological instruments are attached is located 9 m to the north of the pyranometer post. A 9-m-long section of chain-link fence, oriented east–west, is located 18 m south of the pyranometers. The only solid objects that obstruct the horizon in the vicinity of the pyranometers are a small (4-m-long) storage shed and a white propane gas tank adjacent to the shed wall nearest the pyranometers. The building is wood-sided, painted green, and located 12 m west and slightly behind the pyranometers in such a way that direct solar radiation is not blocked at any time of the year.

Based on instrument response factors and horizon obstruction, the error in measurement of combined direct and diffuse solar radiation at the location of the pyranometers is believed not to exceed 5%. The recorded radiation values are 30-min averages, so the incomplete measurement of diffuse radiation (because of the locally obstructed horizon) may be partially compensated for by including radiation reflected by the building and tank to the pyranometers.

Daylength at the site is determined by the height and location of the hills bounding the river valley to the east and west. The highest point of the eastern hill line is ~45 m above the field at a distance of ~520 m. The highest point of the western hill line is ~90 m above the field at a distance of ~460 m. Because of these features, the albedo calculations were limited to that portion of the day when the sun angle was at least 10°.

Before a snow cover is established, the downward-viewing pyranometer measures the radiation reflected by mowed grass. On an overcast day (29 Nov 1990) the albedo of the grass was generally 0.18–0.195, while on the next day, which was sunny (maximum insolation 420 W/m^2 vs. 130 W/m^2), the grass albedo was higher, 0.22–0.25 (Fig. C1). The higher albedo under sunny conditions is consistent with a strong reflection of near-infrared radiation by green vegetation and the higher level of incident near-infrared radiation on the sunny day.

When the ground is snow-covered, approximately 20% of the net solar radiation that penetrates the snow cover to the grass beneath is reflected. With shallow snow covers there is the possibility that the soil beneath the grass will absorb some solar radiation. An indication that this has occurred is a change in temperature of the soil directly beneath the grass. The temperature of the near-surface soil is measured with a copper-constantan thermocouple at a location near the pyranometers where the snow cover intentionally is kept undisturbed. The soil temperature is recorded every 30 minutes. The variation in the near-surface soil temperature on days for which snow albedos were calculated is shown in Figure C2. There can be a pronounced diurnal cycle to the soil temperature, as on 26 Jan, in which the warming
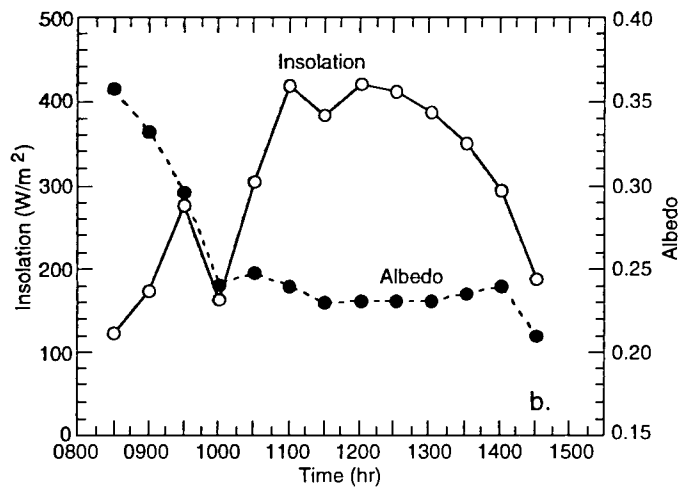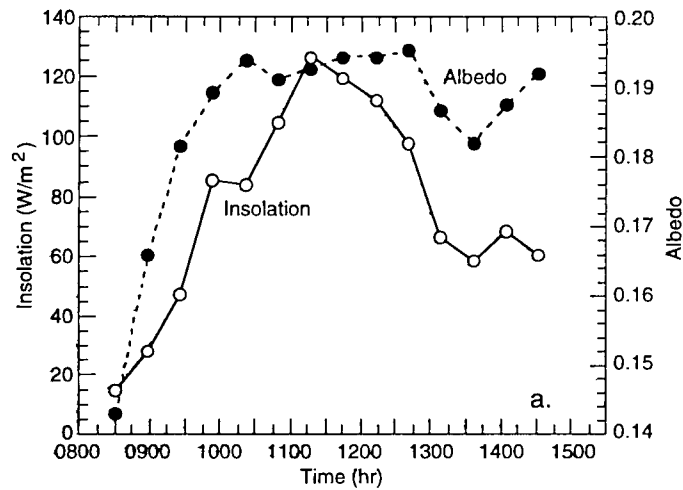
Figure C1. Albedo of prewinter grass cover at SOROIDS on (a) an overcast day (29 Nov 1990) and (b) a sunny day (30 Nov).
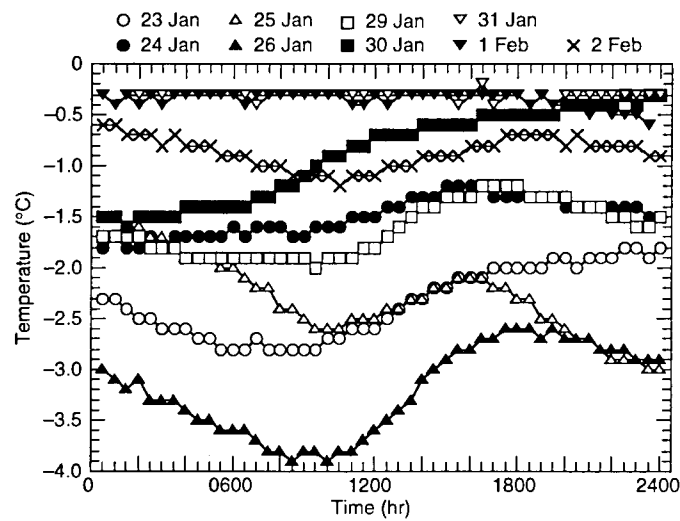

Figure C2. Time-series records of the temperature of the near-surface soil at the base of the grass cover, beneath the snow cover, on selected days in January and February 1991.

26

and cooling of the soil during daylight hours follow, but lag, the changes in insolation. The increase in soil temperature depends on the transmission of solar radiation through the snow, the available radiation after it has been partially reflected by the grass cover, and the thermal properties of the soil. The warming trend is followed by decreasing soil temperatures as the soil radiationally cools in the absence of sufficient solar radiation to maintain the elevated soil temperature.

On 31 Jan, the near-surface soil does not change temperature throughout the 24 hours. Since on this day there was no precipitation after 0330 and the snow surface was cold (Fig. 4), the lack of diurnal variation in soil temperature would not have been the result of percolation of rain or melt water through the snow to the soil surface. It may indicate that with the new snowfall the solar radiation was not penetrating the snow cover sufficiently for a cycle of radiant heating of the soil during daytime followed by cooling at night to occur. Alternatively, the soil temperature may have stabilized at ~0 °C because of contact with melting, ground-heated snow at the base of the snow cover. By 2100 on 1 Feb, a diurnal cycle of soil temperature over the next 24 hours begins to be evident.

REPORT DOCUMENTATION PAGE

1. AGENCY USE ONLY (Leave blank)	2. REPORT DATE August 1994	3. REPORT TYPE AND DATES COVERED

4. TITLE AND SUBTITLE
Variation in Visual and Near-Infrared
Contrast with a Snow Background

5. FUNDING NUMBERS

6. AUTHORS

Lindamae Peck

7. PERFORMING ORGANIZATION NAME(S) AND ADDRESS(ES)

U.S. Army Cold Regions Research and Engineering Laboratory
72 Lyme Road
Hanover, New Hampshire 03755-1290

8. PERFORMING ORGANIZATION REPORT NUMBER
Special Report 94-28

9. SPONSORING/MONITORING AGENCY NAME(S) AND ADDRESS(ES)

Office of the Chief of Engineers
Washington, D.C. 20314-1000

U.S. Air Force Electronic Security
and Communications Center
for Excellence
Hanscom AFB, Massachusetts

10. SPONSORING/MONITORING AGENCY REPORT NUMBER

11. SUPPLEMENTARY NOTES

12a. DISTRIBUTION/AVAILABILITY STATEMENT
Approved for public release; distribution is unlimited.
Available from NTIS, Springfield, Virginia 22161

12b. DISTRIBUTION CODE

13. ABSTRACT (Maximum 200 words)

Visual and near-infrared concealment against a snow cover are considered in terms of the daily and longer-term variation in albedo of a shallow ($\leq$26 cm) snow cover. Examples of albedo of a Vermont snow cover demonstrate the influence of time of day (solar angle), incident solar radiation, snow depth, and snow wetness. Most albedos fell within the range 0.75–0.98. The most consistent variation was a decrease in albedo during the morning as the sun angle increased and a corresponding increase with decreasing sun angle in the afternoon. Albedo was low when the snow surface temperature indicated melting was occurring or when an increase in temperature of the soil beneath the snow cover indicated solar radiation was being absorbed by the soil. Examples of the diurnal variation in sun angle and the seasonal variation in maximum potential solar radiation, as calculated from site latitude and longitude and calendar date, are presented.

14. SUBJECT TERMS

Grass albedo	Snow	Visual concealment	
Near-infrared concealment	Snow albedo	Visual contrast	
Near-infrared contrast	Snow surface temperatures	Wiscombe-Warren model	

15. NUMBER OF PAGES
31

16. PRICE CODE

17. SECURITY CLASSIFICATION OF REPORT	18. SECURITY CLASSIFICATION OF THIS PAGE	19. SECURITY CLASSIFICATION OF ABSTRACT	20. LIMITATION OF ABSTRACT
UNCLASSIFIED	UNCLASSIFIED	UNCLASSIFIED	UL